SWE Stuttgart Wind Energy @ Institute of Aircraft Design

University of Stuttgart
Germany

Research Thesis

Concept Study of a Sailing Offshore Wind Turbine

Leonard Willeke

Supervisor: Prof. Dr. P.W. Cheng
Dr. A. Clifton
MSc. M.Y. Mahfouz

University of Stuttgart
Stuttgart Wind Energy (SWE)
@ Institute of Aircraft Design
Prof. Dr. P.W. Cheng

September 2020 - January 2021

Abstract

Wind turbines play an important role in the transition towards a sustainable future. With the demand for clean energy unbroken, suitable sites onshore become rare and more and more conflicts around land use arise. That's why the industry moved to the sea, where wind resources and space are abundant. After the development of fixed-bottom and floating offshore wind turbines (FOWT), we now present the concept of a sailing offshore wind turbine (SOWT). It can enter deeper waters and will unlock more resources.

The concept builds on the existing spar floating turbines. Specifically, the IEA Wind 15 MW reference turbine and the WindCrete spar are used. Simulations are run in OpenFASTv2.4, while the hydrodynamics of the spar are calculated in Ansys AQWA.
The turbine is not attached to the sea floor but free to move. It is intended to sail with the wind like a ship. The turbine's controller can be used to perform manoeuvres such as stop or turn. The turbine will produce power while sailing. It can store the energy onboard and will unload it periodically, e.g. to ships or stations.
From this approach, many challenges arise. This work focuses on the stability. Special interest lies on the floater's yaw stiffness which is very low. Due to the lack of mooring lines, it plays an important role for the stability. We concentrate on improving yaw stability by the instalment of underwater drag elements that slow down the yaw.
Drag elements lead to a reasonable period of stability. Still, the turbine becomes unstable afterwards. Reason for this is the sideways force $F_{T,y}$, the y – component of the thrust force F_T. It is defined as $F_{T,y} = F_T \cdot \sin \alpha_{yaw}$. The yaw angle α_{yaw} increases constantly under wind load, leading to an increase in $F_{T,y}$ as well. Instabilities occur when $F_{T,y}$ reaches a tipping point but not before. For steady wind with wind speeds v of 20m/s and 25m/s, the following pitch and roll are so strong that the rotor blades touch the water. For the lower wind speeds of 9m/s and 17m/s, pitch and roll are less strong. The turbine can recover and stabilize.

The suggestion is to avoid the tipping point to prevent instabilities. Minimizing $F_{T,y}$ can be achieved by the reduce of the thrust force F_T through rotor blade pitching. Another option is to control the yaw angle α_{yaw} through the nacelle yaw. Both strategies can be implemented into the turbine‘s controller.

Zusammenfassung

Windturbinen spielen eine wichtige Rolle im Wandel hin zu einer nachhaltigen Zukunft. Die Nachfrage nach sauberer Energie ist ungebrochen hoch. Doch Plätze mit guten Windressourcen an Land werden immer knapper. Daher werden nun Anlagen im Meer errichtet, wo Wind und Platz in Fülle vorhanden ist. Nach der Entwicklung von fixierten und schwimmenden Offshore Windturbinen (FOWT) präsentieren wir nun das Konzept einer segelnden Offshore Windturbine (SOWT). Das Konzept baut auf die bestehende schwimmende Anlage mit SPAR-Schwimmer. Es werden die IEA Wind 15 MW Referenzturbine und der WindCrete spar verwendet. Die Simulationen werden in OpenFASTv2.4 durchgeführt, während die Hydrodynamik des SPARs in Ansys AQWA berechnet wird.
Die Turbine ist nicht am Meeresboden verankert sondern kann sich frei bewegen. Sie soll, ähnlich wie ein Schiff, mit dem Wind segeln. Der Controller der Turbine kann verwendet werden um Manöver wie Halt oder Lenken auszuführen. Die Turbine wird während dem Segeln elektrische Energie erzeugen und an Bord speichern. Die Energie wird periodisch abgeladen, z.B. an Schiffen oder Stationen. Dieser Ansatz beinhaltet viele Herausforderungen. Die vorliegende Arbeit beschäftigt sich mit der Stabilität. Besonderes Interesse liegt auf der Steifigkeit des SPAR Schwimmers gegen Scherung, da diese sehr gering ist. Weil Ankerleinen fehlen, spielt sie aber eine wichtige Rolle für die Stabilität. Eine Verbesserung durch das Anbringen von Widerstandselementen unter Wasser wird untersucht.
Widerstandselemente führen zu einer akzeptablen Dauer von Stabilität. Danach wird die Turbine jedoch instabil. Der Grund ist die seitliche Kraft $F_{T,y}$, die y – Komponente der Schubkraft F_T. Sie ist definiert als $F_{T,y} = F_T \cdot \sin \alpha_{yaw}$. Der Scherwinkel α_{yaw} steigt unter Windlast konstant an und führt damit zu einem Anstieg von $F_{T,y}$. Instabilität tritt erst auf, wenn $F_{T,y}$ einen Kipppunkt erreicht. Für stetigen Wind mit Windgeschwindigkeiten v von 20m/s und 25m/s sind die darauffolgenden Roll- und Neigungsbewegungen so stark, dass die Rotorblätter das Wasser berühren. Für die geringeren Windgeschwindigkeiten von 9m/s und 17m/s fallen die Roll- und Neigungsbewegungen weniger stark aus. Die Turbine kann sich wieder stabilisieren.
Es wird vorgeschlagen, den Kipppunkt zu vermeiden, um Instabilitäten zu verhindern. Um $F_{T,y}$ zu verringern, kann die Schubkraft F_T vermindert werden. Dies ist durch die Verstellung des Blattwinkels möglich. Eine andere Option ist die Regelung des Scherwinkels α_{yaw} durch die Drehung des Rotorkopfes. Beide Strategien können mit der normalen Regelung der Turbine durchgeführt werden.

Contents

List of Figures

List of Tables

Nomenclature

Abbreviations

DOF	Degree of Freedom
Fig	Figure
FOWT	Floating offshore wind turbine
MSL	Mean sea level
SOWT	Sailing offshore wind turbine

Symbols

α_{max}	Maximal yaw angle
α_{roll}	Roll angle
$\alpha_{yaw,nac}$	Nacelle yaw angle
$\alpha_{yaw,ptfm}$	Platform yaw angle
$\alpha_{yaw,tot}$	Total yaw angle
α_{yaw}	Yaw angle
β	Decay displacement angle
$\ddot{x}$	Acceleration
$\dot{x}$	Speed
ρ	Density
A	Area
c_d	Drag coefficient
D	Damping
D	Diameter

F	Force
F_D	Drag force
F_T	Rotor thrust force
$F_{T,y}$	y-component of the rotor thrust force
h	Height
I_{XX}	Mass moment of inertia in x-direction
I_{YY}	Mass moment of inertia in y-direction
I_{ZZ}	Mass moment of inertia in z-direction
K	Stiffness
L	Length
M / m	Mass
m_{bal}	Extra ballast mass
m_{tot}	Total mass
N_C	Number of cylinders
T	Wall thickness
t	Time
v_0	Inflow wind speed
$v_{0,rel}$	Relative inflow wind speed for a moving turbine
v_{rated}	Rated wind speed
v_{rel}	Relative flow speed
$v_{sailing}$	Sailing speed
x	Displacement
z_{grav}	Height of the center of gravity

Chapter 1.

Introduction

1.1. Motivation

With global temperatures rising, the need for sustainable energy is unbroken. To transform the price-driven energy market, emission-free power must be delivered at the same cost as conventional sources. One of the biggest parts of renewable electricity comes from wind turbines. With better wind resources and more space offshore, the industry is moving to construct more and more wind parks in the sea. While turbines with fixed foundations, driven into the seafloor, are common today, a new technology is embarking. After decades of research on the topic, floating offshore wind turbines (FOWT) are on the brink of commercialisation. Their most notable advantage is the possibility to be anchored in deeper waters, where foundations are to expensive or not feasible. Still, most of the ocean‘s surface remains unused although most wind resources can be found here. This is due to deep waters that forbid foundations or anchoring and the inability to transmit the produced energy to consumers on the mainland.
To effectively use the high seas to harvest wind power, an unmoored swimming system is needed that can convert the power and store the wind energy. Few ideas have been presented on this topic. They include an early proposition of a treadmill-powered boat (Vidal [U.S. Patent 4 371 346, Aug. 1980]) and the recent idea of energy ships using Flettner rotors (Babarit et al. [2020]).
However, none of the concepts builds on the research of floating wind turbines. Our proposition is to adapt a floating 15 MW turbine based on a SPAR platform. The SPAR is in use for offshore applications since decades and has been used for the first floating offshore wind park HyWind as well (see eg. Skaare [2017]). Models of the turbine and the platform in the simulation program FAST (NREL ™) are used for testing. The focus is on the stability of the system when used without anchoring. The question of energy storage is not discussed.

1.2. Note on methodology

This research work was organized after the SCRUM framework. Details can be found in the guide by Schwaber and Sutherland [2017]. It is based on the idea of incremental development and focuses on usability. This means that progress is packed into encapsulated stages that represent a useful result on their own.

The backbone of SCRUM is a division of responsibilities between the positions of Scrum Master, Product Owner and Development Team. The Scrum Master provides insight on the organizational methods described by Schwaber and Sutherland [2017]. The Product Owner is responsible for the end result and helps the Development Team clarify their goals. The Development Team consists of the people doing the actual research. They are self-organized and work with a high level of autonomy. This ensures the focus on usable results in a development under uncertainty. Here, goals are prone to change as you learn more about the subject.
During the research, my two supervisors took on the roles of Scrum Master and Product Owner while I, the student, was the sole member of the Development Team.
The report at hand adopts the idea of encapsulated progress. The name of each chapter is a question that needed to be answered as the research went on. The chapters include all the information necessary to do so. Traditionally, the content would be split up in different sections, eg. “Methods” and “Results”. Nevertheless, the chapters build upon each other as the answers to one question lead to the next question. The use of SCRUM allowed for a dynamic research that adapted to the results at hand.

Chapter 2.

Can the original spar be used for a sailing turbine?

Throughout this work, we will use the IEA Wind 15 Megawatt Offshore Wind Turbine model as described by Gaertner et al. [2020]. The 15MW turbine with a rotor radius of 120m has a hub height of 135m above Mean Sea Level (MSL). The WindCrete model from Mahfouz et al. [2020] is used as spar platform. Its cylindrical structure has a diameter of 18.60m except for a transition cone to the tower at the top and a sphere bottom. The whole construction reaches a depth of 155m relative to MSL. The tower holding the turbine is also described by Mahfouz et al. [2020]. The coordinate system used is shown in Fig. 2.1. As initial position, the turbine is facing upwind while the x-axis points downwind.

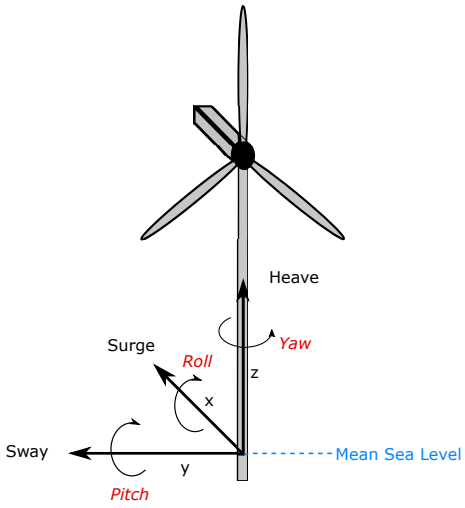

Figure 2.1.: *Coordinate system*

From an engineering point of view, the re-use of the well-established spar platform would be ideal. It has been tested extensively in the last decades and is known to withstand the harsh offshore conditions (Henderson et al. [2016]). Besides, by using a standardized platform that works in floating as well as in sailing concepts, a turbine could be used in both applications interchangeably. Cost reduction by

mass production is also important. However, we would expect to implement some changes in the turbine for a sailing use case, at least in the controller software. To start with this scenario, we will look at a spar with its mooring lines removed.

2.1. How does a spar behave without mooring?

A spar is nothing more than a tall buoy. As such it is stiff against pitch, roll and heave, meaning it will try to return to its respective initial position after a displacement. This is due to the distribution of mass and inertia in the platform. For surge, sway and yaw the spar is not stiff. Normally stiffness is provided by the mooring lines. When the mooring lines are removed, the turbine can be expected to move freely in yaw, surge and sway but not in pitch, roll and heave. To test the response, the simulation depicted in Fig. 2.2 is computed. A loose system is simulated under a steady wind with wind speeds of $v_0 = 6, 10.59$ and 25m/s. The Degree of Freedom (DOF) of the nacelle yaw is turned off. There are no waves and no currents.

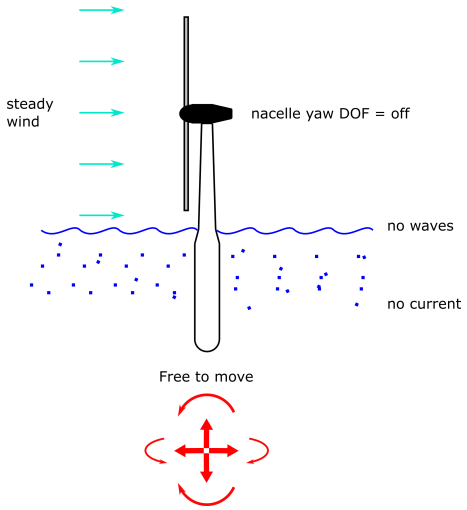

Figure 2.2.: *Simulation case*

The simulation results in Fig. 2.3 show unexpected strong movements for wind speeds $v_0 \geq v_{rated} = 10.59$m/s. Notable motions are marked by red arrows. Surge changes rapidly after a period of constant change. For $v_0 = 25$m/s a slight drop occurs. Sway starts to change fast around $t = 60$s, this time with a fall for $v_0 = 10.59$m/s. Pitch and roll change rapidly after a period of almost no change. Yaw is rising constantly until its curve, too, gets steeper.The turbine is rotated from front to back. It's remarkable that only the simulation for $v_0 = 6$m/s runs for the full time of 200 seconds. For $v_0 = 25$m/s and $v_0 = 10.59$m/s the simulation stops before reaching the end due to the strong movements. The loose system is

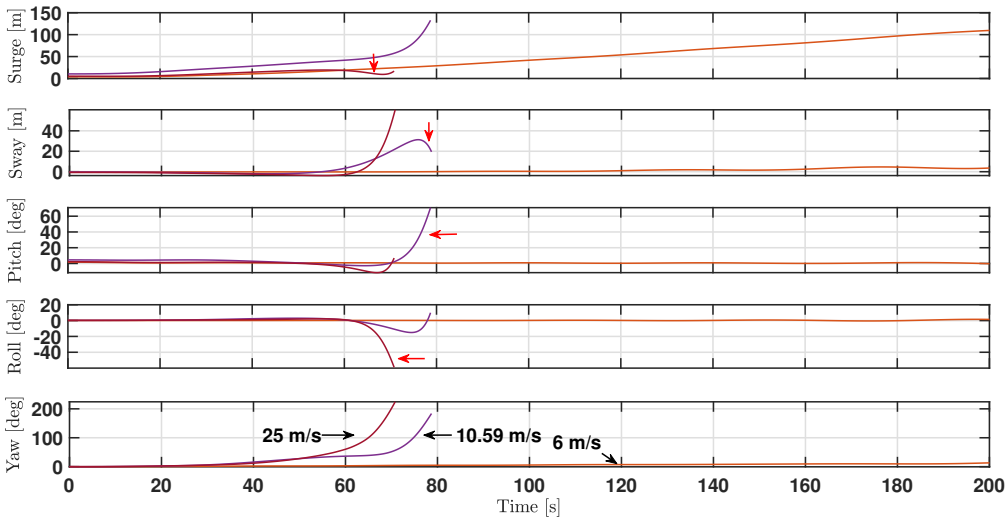

Figure 2.3.: *Movements for a spar without mooring in wind speeds* $v_0 = 6$, 10.59, 25m/s. *The turbine is very unstable with extreme motions in all DOF. The red arrows mark notable motions. Not expected were the strong pitch and roll as well as the negative surge and sway.*

clearly unstable for high wind speeds. This is not practical, as high wind speeds yield the most power. Problematic is also the yaw motion, spinning the rotor constantly out of the wind. The drops in surge and sway are noteworthy as the turbine changes its direction and moves towards the wind.
In Fig. 2.4 the yaw is fixed at $\alpha_{yaw} = 0\,\text{deg}$. This is done to test the influence of the yaw on the instabilities. Unlike before, the curve characteristics are similar for every wind speed v_0. Surge and sway now proceed constantly with no big disturbance or drop. Pitch and roll oscillate between moderate values as expected for the stiffness of the spar. This indicates that stabilizing the yaw is important for the stability of the turbine.

To conclude, a spar without mooring lines is very unstable. Prevention in form of a stabilized turbine yaw seems effective. Besides, the phenomenon of surge and sway towards the wind sparks interest. If this behaviour could be replicated and controlled, the sailing turbine could be steered properly.

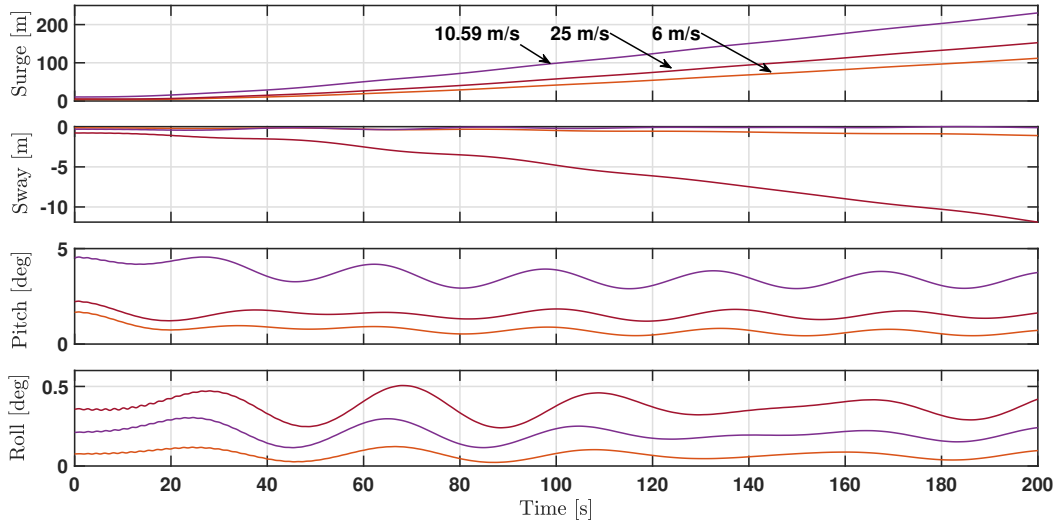

Figure 2.4.: *Movements for a spar without mooring and fixed turbine yaw* $\alpha_{yaw} = 0°$ *in wind speeds* $v_0 = 6,\ 10.59,\ 25$ *m/s. The turbine is stable.*

2.2. Can you sail against the wind?

A sailing turbine will encounter situations in which going backwards, towards the wind, would be best. Negative surge and sway is observed for great yaw angles in Fig. 2.3 but not in Fig. 2.4 where yaw is fixed at 0 deg. This fosters the idea that wind inflow on the backside of the rotor blades is involved. Inflow on the front side leads to a thrust force in wind direction (see e.g. Manwell et al. [2009]), pushing the turbine forward. Inflow on the rotor blade backside seems to create thrust opposite to the wind direction. To test this, turbines with different great yaw angles are simulated in steady wind with $v_0 = 10.59$m/s. Surge and sway, shown in Fig. 2.5 and Fig. 2.6, indeed show movement towards the wind inflow direction. But the motions are very rapid and impulsive. Also, the simulation still fails. The failures occur during the fast motion of either surge or sway, indicating that the turbine suffers great forces. This needs to be avoided in a real system but would be hard to control. The fast and impulsive surge and sway motions therefore scatter the idea of actively sailing against the wind.

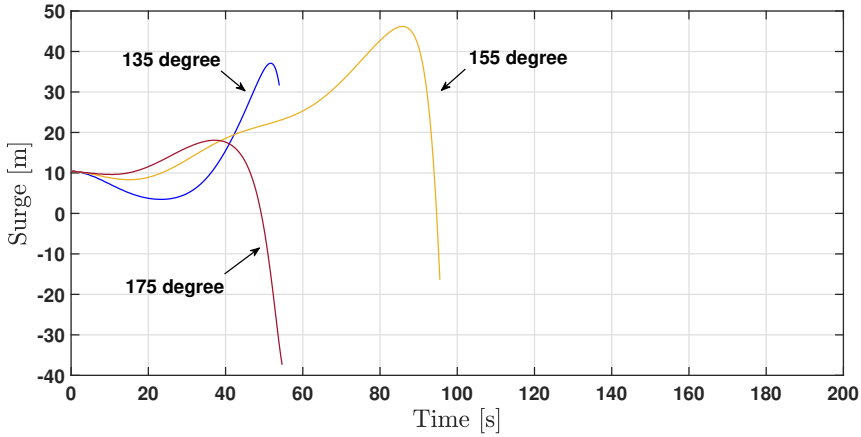

Figure 2.5.: *Surge for big initial yaw angles α_{yaw} where the wind inflow hits the rotor blade backside. Surge towards the wind is observed but always with very fast motions.*

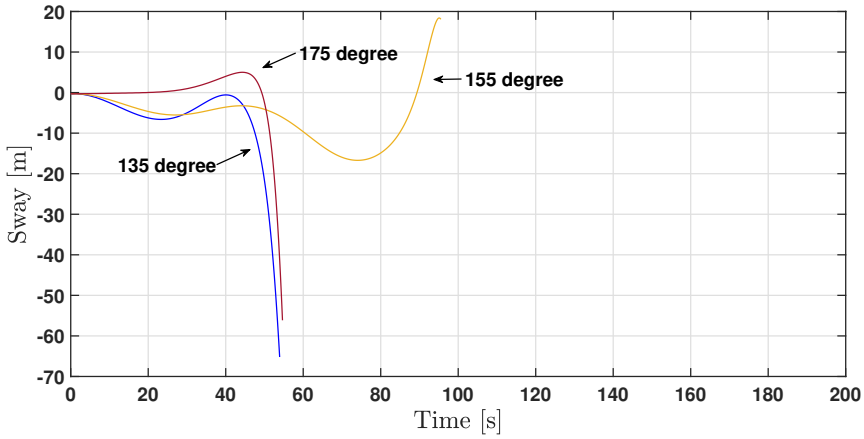

Figure 2.6.: *Sway for big initial yaw angles α_{yaw} where the wind inflow hits the rotor blade backside. Sway towards the wind is observed but always with very fast motions.*

But what about yaw towards the wind? Yaw is a big problem in stabilizing the turbine. If the rotor blade backside would produce yaw towards the wind, this could be used to keep the rotor faced to the wind. This is actually the case, as Fig. 2.7 displays. A negative initial yaw angle induces positive yaw while a positive initial yaw angle induces negative yaw. Besides, the figure shows that higher wind speeds lead to an earlier extreme yaw and an earlier stop of the simulation. But like surge and sway, the rise in yaw occurs rapidly. In combination with the following simulation failure this makes the use of yaw towards the wind very hard to control and will not be followed further.

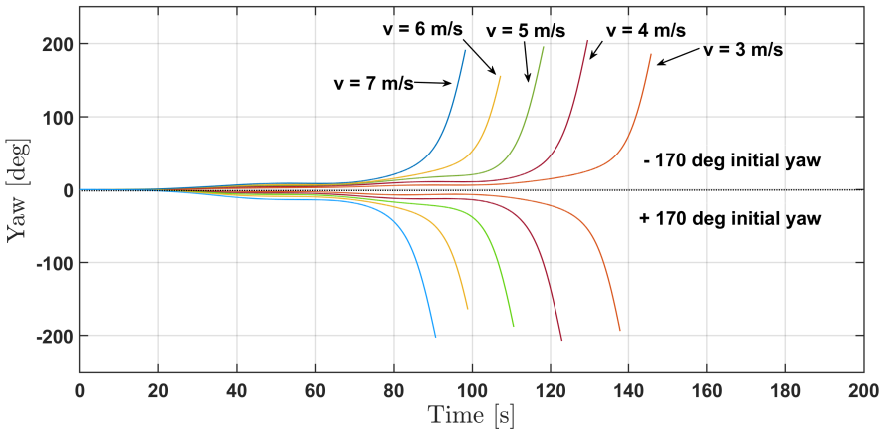

Figure 2.7.: *Platform yaw for positive and negative big initial nacelle yaw angles $\alpha_{yaw,nac}$. The rotor is positioned and the nacelle then fixed on the tower. The wind inflow hits the rotor blade backside causing platform yaw towards the wind. For higher wind speeds, the turbine yaws earlier.*

2.3. Can you stabilize the spar just by nacelle yawing?

Unregulated turbine yaw destabilizes the turbine. Therefore, a method to counter the wind-induced yaw is needed. One approach is to use the nacelle yaw. As the nacelle can rotate with up to $2\,\mathrm{deg}/s$, it is able to outrun the platform yaw. The total yaw made by the sum of both yaw angles could be kept at any angle. By this, a method to stabilize and steer the turbine would be provided.

A simplified version of this approach is shown in Fig. 2.8. A comparison run without yawing is colored red. The blue and yellow curve show a turbine with a nacelle yawing in negative and positive angels, respectively. The simulation run with $v_0 = 10.59\mathrm{m/s}$ unveils that nacelle yaw leads to platform yaw in the opposite direction. An explanation for this is the moment created by the motor rotating the nacelle. It acts on the turbine tower and therefore also on the platform which starts to rotate opposite to the nacelle. But because the spar platform has a cylindrical shape, there‘s neither enough friction nor inertia to slow the platform yaw down. The spar spins faster than the nacelle. The total yaw $\alpha_{yaw,tot} = \alpha_{yaw,nac} + \alpha_{yaw,ptfm}$, which is the sum of nacelle and platform yaw, shows this clearly. Yawing the nacelle destabilizes the turbine and leads to a faster stop of the simulation. A stabilization purely by nacelle yaw control seems therefore very unlikely and hard to implement. Another method is needed.

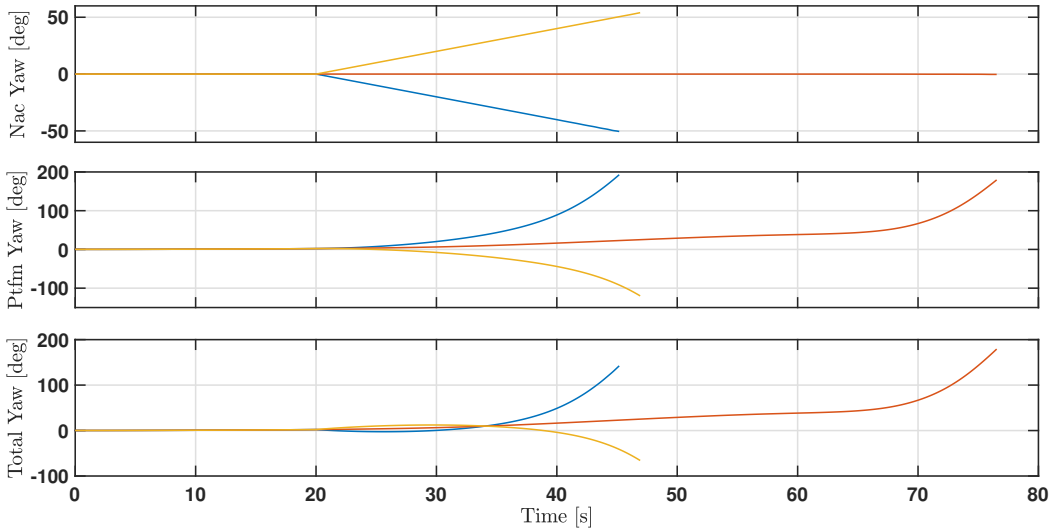

Figure 2.8.: *Influence of the nacelle yaw on the total yaw. The wind speed amounts to* $v_0 = 10.59\text{m/s}$. *Yawing the nacelle creates a moment on the platform. This moment is strong enough to rotate the platform as seen in the second graph. The total yaw is defined* $\alpha_{yaw,tot} = \alpha_{yaw,nac} + \alpha_{yaw,ptfm}$. *It is dictated by the induced platform yaw which is faster than the original nacelle yaw. This is probably due to little friction and inertia of the spar.*

2.4. How good is the power curve of an ideal sailing wind turbine compared with fixed and floating turbines?

It has been shown throughout this chapter that a sailing wind turbine based on a spar is not stable and will take further modifications to work. One could justly pose the question if the concept is worth the trouble. How much power output can be expected, and at what wind speeds? To answer this, the power curve is simulated under ideal conditions. 'Ideal' for a sailing turbine means that the rotor is always facing the wind while it gets dragged through the ocean. Naturally, a moving turbine would need to make course adjustments like limiting speed or yawing the rotor to steer. But we neglect any situations that would require the turbine to limit its power output and compare only the ideal case with traditional concepts.

The comparison in Fig. 2.9 illustrates that the sailing spar concept is less efficient than a fixed or floating turbine, even under ideal conditions. The rated wind speed is $2m/s$ higher, the course of the power curve following roughly the path of its competitors in shape. This is reasonable as the turbine is moving with the wind, decreasing the relative inflow wind $v_{0,rel} = v_0 - v_{sailing}$ by its own speed.

Hence a sailing turbine will always need higher wind speeds to obtain the same power output as its competitors.

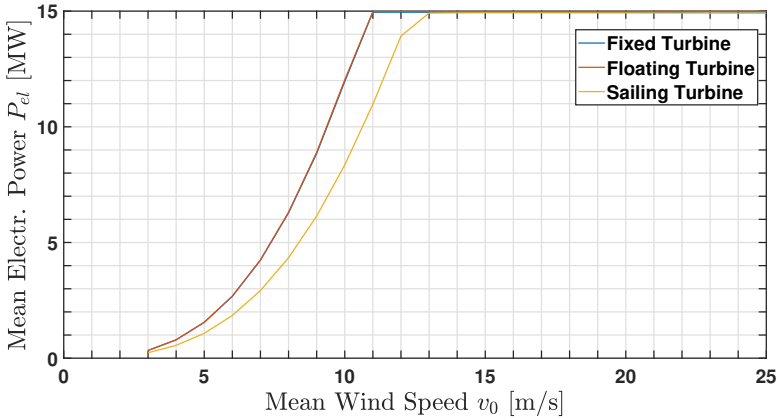

Figure 2.9.: *Comparison of the power curves of a fixed, a floating and a sailing turbine. The rotor of the sailing turbine is always facing the wind to simulate ideal conditions. Fixed and floating turbine have almost exactly the same power curve. Power output of the sailing turbine is lower as it moves with the wind, decreasing the relative wind inflow speed.*

Although a sailing turbine is producing less power than the conventional alternatives, it's still competitive. The exact power output in the field will depend very much on the conditions of operation. For now, the concept has proven its abilities.

Chapter Summary

In this chapter we set out to ask whether it is possible to use the original spar platform with no modifications as basis for a sailing turbine. It became clear that we can not just cut a spar turbine loose and let it sail over the seas. It yaws immediately when the wind starts to blow, driving the rotor out of the wind. The simulations unveiled a striking instability and a pitch and roll behaviour that can only be described as extreme. Besides, the very attempt to take control over the turbine by yawing the nacelle is spoiled by a spar platform that has no means to resist against rotation. We learn from this that our first and foremost task is to stabilize the platform in the water, giving it some resilience against the forces acting on it. If we can do this, the open seas with its abundant resources in wind and space could be harnessed with competitive efficiency.

Chapter 3.

How can we stabilize the turbine?

As seen in chapter 2, the problematic degree of freedom is the yaw. Pitch and roll may oscillate in a reasonable range before spiking to extreme values. But this behaviour disappears when the yaw is fixed and the rotor always faces the wind. To stabilize the turbine means to limit the yaw.
Yaw is created by the forces acting on the turbine. The linear Equation of Motion

$$[\mathbf{M}] \cdot \ddot{\mathbf{x}} + [\mathbf{D}] \cdot \dot{\mathbf{x}} + [\mathbf{K}] \cdot \mathbf{x} = \mathbf{F}, \tag{3.0.1}$$

(see e.g. Faltinsen [1993]) describes the relationship between a force F and the displacement x, speed $\dot{x}$ and acceleration $\ddot{x}$ that result from it. The matrices $[M]$, $[D]$ and $[K]$ represent mass, damping and stiffness, respectively. For a sailing wind turbine the stiffness K must be zero, as the system is loose and free to move. Damping D is determined by the geometry of the platform and its hydrodynamic properties. Increasing D or K will limit the displacement and speed caused by a force F.
But how can stiffness and damping be changed in the simulation and how effective are they in reducing the yaw? FAST provides an input for the stiffness matrix K. Thereby the model can be adapted formally, only in the calculation, with no change in geometry. Only the (6,6) entry is changed to simplify. Damping can be increased by changing the geometry. Here FAST provides the option to add cylinders to the initial body for which drag is calculated. Drag is only a part of damping which includes many more hydrodynamic forces. But to calculate these is a long and tedious process, unfit for fast iteration. The drag force gives a good first glance if a design is fit to be used for our case.

Figure 3.1 compares the yaw behaviour of a spar without modification with the results for a platform with modified stiffness values and attached cylinders. The load case is simple: the nacelle of the turbine is rotated 180 degrees by a motor, causing a moment on tower and platform.

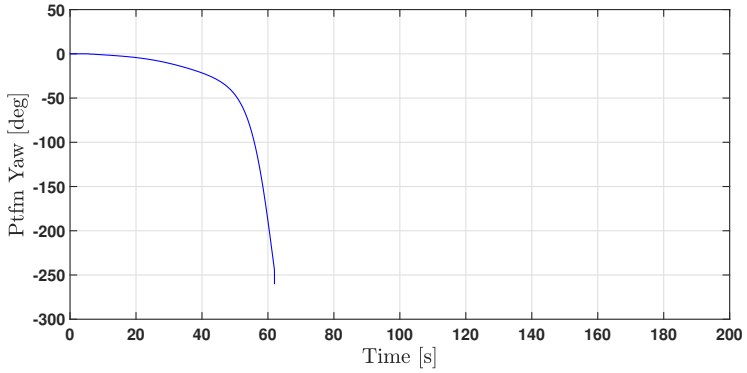

(a) Spar without modification

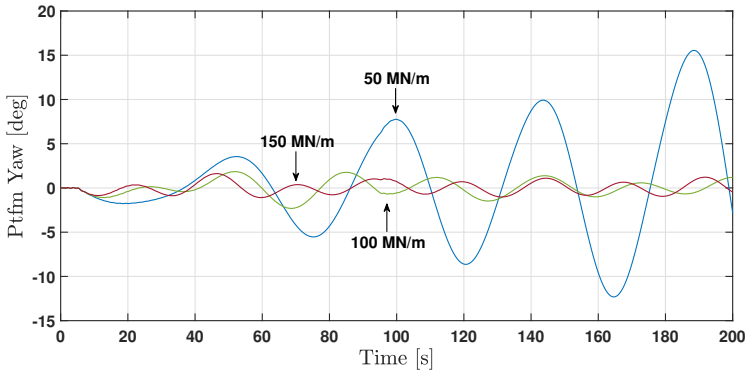

(b) Spar with modified stiffness matrix

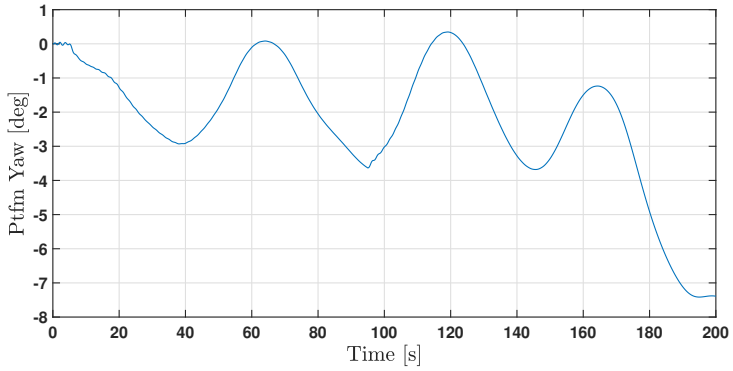

(c) Spar with attached cylinders

Figure 3.1.: *Yaw reaction of different stabilization methods on a nacelle yaw of* 180 deg

An unmodified spar (Fig. 3.1 a)) is so unstable that the motor moment is enough to cause heavy yaw and a stop of the simulation.
The approach to modify the stiffness (Fig. 3.1 b)) shows better results. The stiffness has great impact on the platform yaw: a higher value corresponds to some extend with a heavier constraint on the rotation. The turbine can be stabilized with this very well. The yaw is kept small and oscillates around 0 degree for high stiffness values. The problem with this approach is that stiffness can not be provided by something that is attached only to the moving platform. A connection to the immobile surrounding would be necessary. But that's against the whole idea of a loose turbine which is why we abandon this solution.

Consider now the cylinder method. If we attach horizontal cylinders to the spar like in Fig. 3.2, they get pushed through the water as the platform rotates. The following drag forces act in the opposite direction, causing the turbine to slow down. To reach a stable condition, the drag forces must be high enough. In Fig. 3.1 c), two cylinders with a length of $L = 100$m and diameter $D = 10$m are attached at each side of the spar parallel to the platform x-axis. The cd - value of the cylinders is set to 1. This modification improves the stability by much. It provides us with a method to increase stability while keeping the turbine loose. Now, of course, the question is if the damping effect is sufficient and how exactly the cylinders have to be designed.

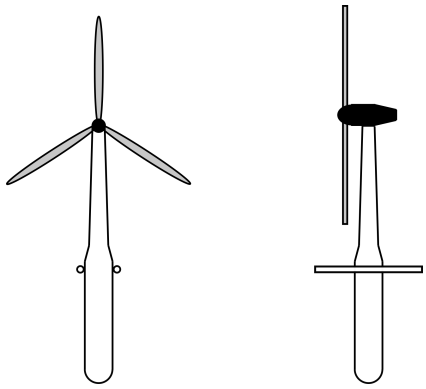

Figure 3.2.: *Spar with two horizontal cylinders attached.*

Chapter 4.

Can the turbine be stabilized through attached cylinders?

As seen before, the installation of horizontal cylinders does have an effect on the stability of the turbine. We will now investigate which design options we have and whether a fully stable state can be reached by this method.

4.1. Which cylinder parameters are important and how should they be chosen?

It is important to remind ourselves that we model the cylinders only by the drag forces they create. For now, the bodies have no inertia and don‘t induce any other hydrodynamic forces. Therefore, it is easy to see which parameters will have an impact on the platform movement.

The hydrodynamic drag force F_D acting on a cylinder in a fluid is expressed by the formula

$$\mathbf{F_D} = \frac{\mathbf{1}}{\mathbf{2}} \cdot \rho \cdot \mathbf{v_{rel}^2} \cdot \mathbf{c_d} \cdot \mathbf{A} \tag{4.1.1}$$

(Journee and Massie [2001]). Here, v_{rel} is the relative speed between the body and the fluid. Drag force will be induced either if the cylinder moves through the water or a water stream moves around the cylinder. To capture the space the body is blocking while moving through the fluid, area A is the space the body has perpendicular to the direction of v_{rel}. In case of a cylinder with inflow on the long side, the flow only "sees" a rectangle. Therefore A is given by the length times the diameter of the cylinder or $A = L \cdot D$. The constant c_d characterizes the surface and geometry of the body and is usually $c_d = 0.7$ for a cylinder with a smooth surface. The density of water is given as $\rho = 1025\text{kg/m}^3$.

Formula 4.1.1 reveals several options to increase the drag force and reduce the yaw accordingly. For a start, the cylinder should be as long as possible to increase the area A. The same is true for the diameter D. Also, if the c_d is adaptable, it should be high as well. One parameter that‘s not exactly shown is the number

of cylinders attached to the spar. Installing more cylinders will increase the total drag force.
Testing the different geometry options in the simulation brings unexpected results. Despite having the same area A and everything else being equal, a long, slender cylinder and a short, thick cylinder lead to different yaw reductions. The long cylinder does better than the short one. This is probably due to the squared relative velocity v_{rel}^2 in the term for F_D. When the platform yaws, the speed of each cylinder segment depends on how far away it is from the rotation axis. The outer ends of a cylinder therefore experience more drag than the inner segments. In addition, the outer segments have a greater lever on the platform and act with a bigger moment against the yaw than inner segments. The same reasoning can be used to decide whether the cylinders should be oriented horizontal or vertical. A vertical cylinder will reach lower segment speeds and not make use of the lever as a horizontal cylinder. This leaves the vertical version with a much greater area to achieve the same yaw reduction.

4.2. Which substructure design works best?

Of course, there are many designs that conform to the requirements above. We are aiming for a structure that is realistic to manufacture and slows down the yaw sufficiently to stabilize the platform. In order to compare different designs, we first have to define what "sufficient" means in this context. We define a load case of yawing the nacelle about 180° with no wind inflow. Every design will be adapted to restrict the platform yaw to a maximum of $\alpha_{max} = 5° \pm 0.3°$ during the simulation time of $t = 200$s. We can then compare which parameters are necessary. We set the c_d to $c_d = 5$ and the diameter to $D = 5$m for all cylinders. Now the length of the cylinders is the only parameter left. The designs differ in their number of cylinders and the way they are positioned as shown in Fig. 4.1. To take the number of cylinders N_C into account, the area $A = N_C \cdot L \cdot D$ is used to compare. Less area for the same yaw reduction means we have to use less material to reach the same result.
Table 4.1 holds the results for the comparison. It becomes clear that the moment created by the drag governs the yaw response. Although a design with eight cylinders can use quite short obstacles, the total area needed is much larger than for designs with fewer, longer cylinders. This means more material to be used. On the other hand, attaching only one cylinder makes good use of the material but already seems to operate at its limit. Remember, the only force applied is the yaw moment of the nacelle and this design needs a cylinder with almost a hundred meter length to counter that. Expanding the tube further for bigger loads like wind will be challenging. Therefore we think that the designs with two and four cylinders present a good trade-off between material use and length. We choose the design c) with four cylinders as it gives us the most margin to act.

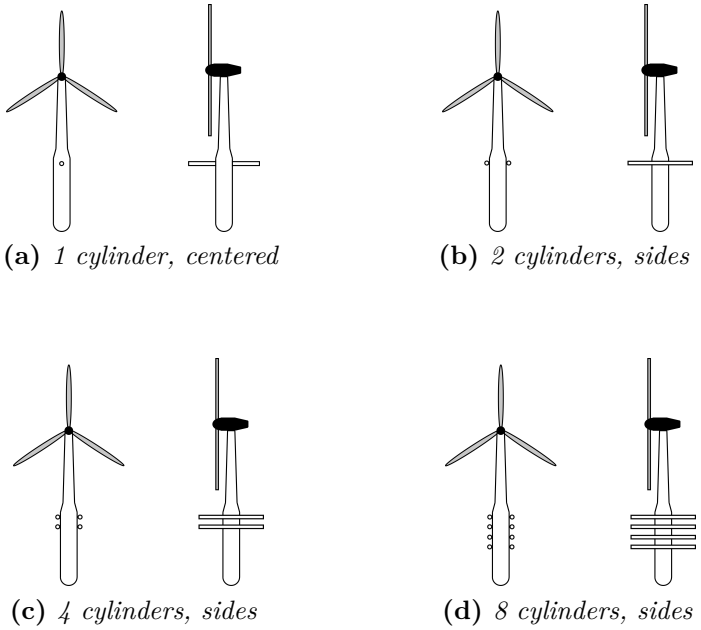

(a) *1 cylinder, centered* **(b)** *2 cylinders, sides*

(c) *4 cylinders, sides* **(d)** *8 cylinders, sides*

Figure 4.1.: *Different platform designs with drag cylinders. The cylinders are installed at heights* $z = [-15\text{m}, -35\text{m}, -55\text{m}, -75\text{m}]$ *relative to MSL, respectively.*

Number of cylinders	1	2	4	8
Length per cylinder [m]	95	76	66	53.7
Total Area [m^2]	475	760	1320	2418

Table 4.1.: *Cylinder geometry to limit the platform yaw to* $5^\circ \pm 0.3^\circ$ *during nacelle rotation. Constant values are* $D = 5\text{m}$ *and* $c_d = 5$ *for all versions. Cylinder length decreases with more cylinders but total area* $A = N_C \cdot L \cdot D$ *increases. This is because cylinder sections further away from the rotation axis, which lies in the spar, experience higher drag and have a bigger lever.*

One further adaption has to be made before we test the design on wind loads. Currently the cylinders are all parallel to the x-axis of the platform coordinate system. This is unimportant during the nacelle yaw example where the turbine doesn‘t move. But under wind, when the platform ploughs through the ocean, it matters how the cylinders are directed. The forward motion creates a drag force as the platform moves through the water. With parallel cylinders only, the drag created isn‘t equal for all direction. This leads to more platform yaw. To prevent this, the four cylinders are arranged in a cross layout as shown in Fig. 4.2.

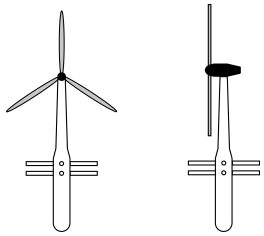

Figure 4.2.: *Improved four cylinder design. The cross layout should prevent a rotation from drag created through forward motion.*

4.3. Is the turbine stable now for wind load?

Our platform is now adapted to withhold the moment acting during nacelle yaw. The underwater drag forces are big enough to hold it from unstable movements. Therefore we can finally turn towards a case with wind load. While the nacelle yaw moment acted only for a defined and short time, the wind is acting for the whole simulation. The turbine is continuously experiencing loads.
We see that the movements improved with the new design. They are slower and the platform seems to withstand the forces for some time. But then rapid movements appear again, the same as before, leading to a crash.
In an attempt to get better results, we exhaust the design margin we have which improves the behaviour a little. The new parameters are listed in Tab. 4.2 and will be used from here on. The drag coefficient of $c_d = 100$ is unrealistic for a cylinder but used for now. This is done in order to test the concept of stabilization by drag elements. Still, the turbine is very unstable under wind load.

Length L	100 m
Diameter D	5 m
Drag coefficient c_d	100

Table 4.2.: *Final design parameters for the cylinders*

Although we adapted the design by adding big drag elements, this is not enough to stabilize the turbine under wind load. We have to take one step back and look at the reason of the instability in order to adapt the platform design accordingly.

Chapter 5.

Why exactly does the simulation fail and how can it be avoided?

To understand the instabilities of the system, the sailing turbine is simulated under steady wind conditions as seen in Fig. 5.1 . The four-cylinder platform with a cross layout and cylinder parameters $L = 100\text{m}$, $D = 5\text{m}$ and $c_d = 100$ is used. The rotor is facing upwind at the start with the nacelle yaw DOF turned off, but the platform is free to yaw and move. Wind speeds from a wide range are applied, four of which are chosen to display the behaviour throughout this chapter. Initially, a period of $t = 1500\text{s}$ is simulated during which the simulation fails for several wind speeds.

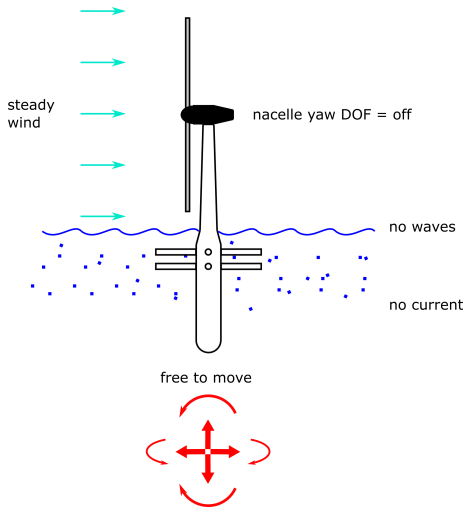

Figure 5.1.: *Simulation case*

5.1. Why does it fail under wind load?

A look in the error messages provided by FAST reveals that the cause for the simulation failure is the rotor blades touching the water surface. The turbine

pitches and rolls so much that the long blades dip into the sea. To display this, Fig. 5.2 shows the pitch, roll and yaw of the turbine for $v_0 = 9, 17, 20, 25\text{m/s}$. While yaw increases steadily from the start for all wind speeds, pitch and roll stay low. But then both values peak simultaneously at a different time for each wind speed $v_0 \geq 17\text{m/s}$. In case of $v_0 = 20\text{m/s}$ and $v_0 = 25\text{m/s}$, they cause the simulation to stop. For $v_0 = 17\text{m/s}$ pitch and roll are heavy, too, but not enough to bring the rotor blades to the water surface. Only for the lowest simulated wind speed $v = 9\text{m/s}$, no instability occurs.
During simulation the incoming wind speed does not change over time, but the state of the turbine does. Also, higher wind speeds contribute to a faster rise in yaw and simulation stop.

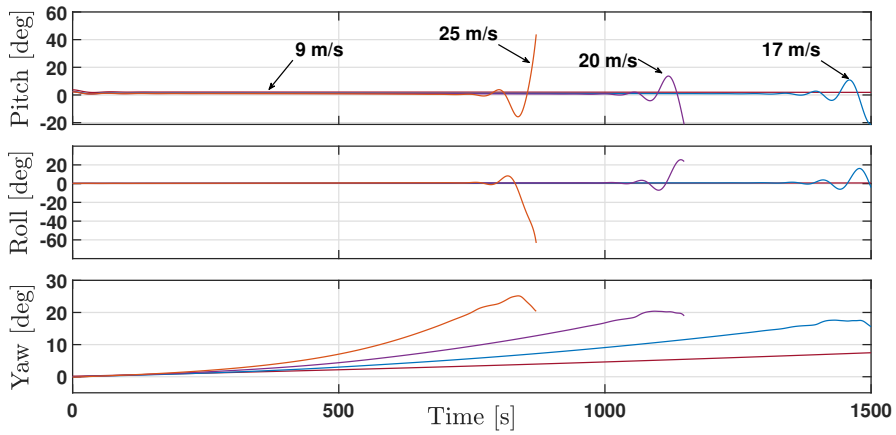

Figure 5.2.: *Movement of the turbine under wind load. Pitch and roll first stay low, then peak fast. Yaw increases steadily. Higher wind speed causes faster yaw and earlier peaking. Peaks are accompanied by simulation stop due to the blade tips hitting the water surface.*

5.2. Why does it pitch and roll so much and only after some time?

The time span between simulation start and instability in pitch and roll suggests that some force has to build up. This would be typical for the coupling of natural frequencies (Gasch et al. [2012]). If the natural frequencies of yaw, pitch and roll would be coupled, the exposure to wind load could lead to increasing oscillation. To check on this hypothesis, decay tests are made. After an inital displacement of $\beta = 5°$ in the respective direction the structure is left to regain a stable state. The results in Fig. 5.3 show that pitch and roll share the same natural frequency. This is usual for a SPAR and expected for our design as the platform is symmetric along the x- and y-axis. An excitation will therefore be met with similar inertia,

damping and stiffness.
What about the yaw natural frequency? The decay test shows that it lies in the same range as for pitch and roll. But deeper thought should warn us about this result: The natural frequency measures how a system, when excited once, will swing forth and back on its own. For a loose turbine the yaw simply has no restriction from going further into one direction, it has no stiffness. It won‘t swing back. Therefore, the decay test result for yaw is misleading.

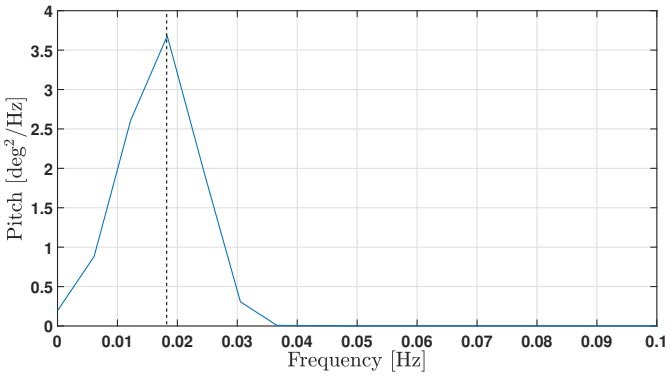

(a) Pitch frequency result for an excitation of 5°. The natural frequency is 0.0186Hz.

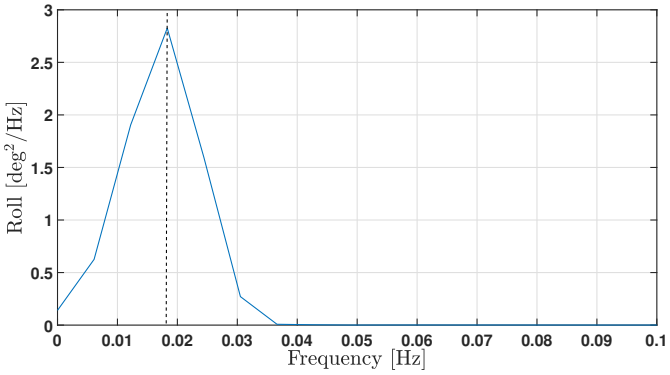

(b) Roll frequency result for an excitation of 5°. The natural frequency is 0.0186Hz.

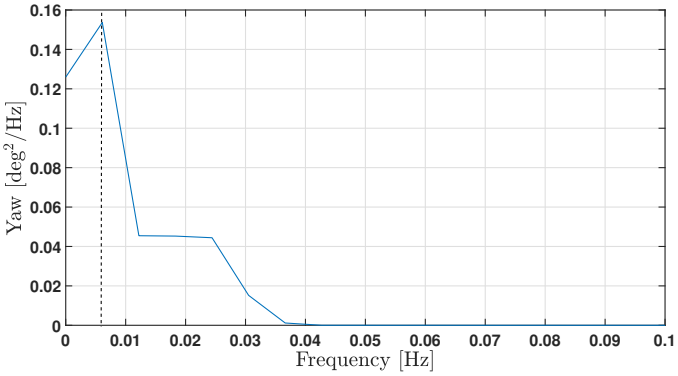

(c) Yaw frequency result for an excitation of 5°.
The result is invalid as the turbine is free to move in yaw direction.

Figure 5.3.: *Frequency results of the decay tests for pitch, roll and yaw*

We need to make more observations to solve this problem. How exactly is the turbine behaving in Fig. 5.2? While pitch and roll don‘t change much for most of the simulation time, yaw is consistently increasing. Then at some seemingly random point, pitch and roll start to change rapidly and lead to the break. What if the yaw angle had an influence on the pitch and roll behaviour?
Exactly this case is presented by Haslum et al. [2020]. As laid out there, roll and yaw are connected by the thrust force in two ways. First, yaw enhances roll as shown in Fig. 5.4. The assumption is that for small disturbances of the yaw angle α_{yaw}, the thrust force is still perpendicular to the rotor plane. The thrust force is then no longer parallel to the x-axis. Instead it has a component $F_{T,y}$ parallel to the y - axis. It is calculated by the simple formula

$$\mathbf{F_{T,y}} = \mathbf{F_T} \cdot \sin \alpha_{\mathbf{yaw}} \tag{5.2.1}$$

$F_{T,y}$ causes the turbine to swing along the y-axis, or in other words roll. We can say that yaw induces roll. Second, roll also enhances yaw. See Figure 5.5 for this. When the turbine rolls, the thrust force suddenly has a lever L to create a moment along the z-axis. The size of L is determined by $L = h \cdot \sin \alpha_{roll}$. Thereby, roll creates yaw. We see that roll and yaw are connected by the thrust force.

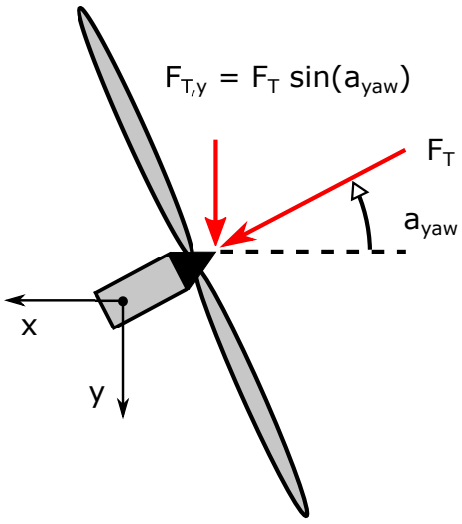

Figure 5.4.: *Coupling of thrust force F_T and roll by the yaw angle α_{yaw}. The yaw allows the thrust force to increase the roll over the component $F_{T,y}$. Figure recreated after Haslum et al. [2020].*

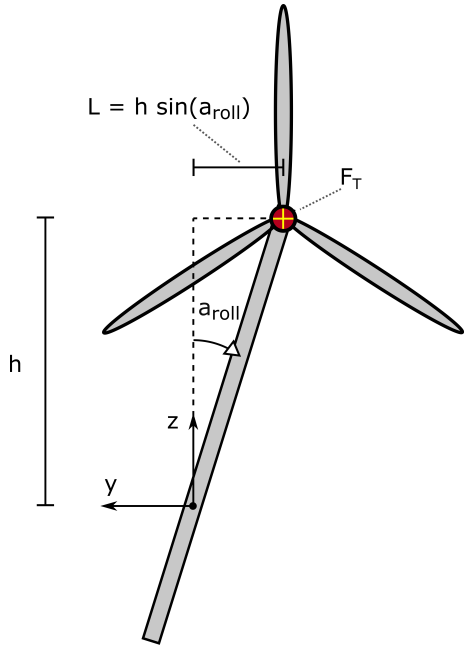

Figure 5.5.: *Coupling of thrust force F_T and yaw by the roll angle α_{roll}. The lever L allows the thrust force to increase the yawing of the platform. Figure recreated after Haslum et al. [2020]*

For a loose turbine, movement in roll and yaw is inevitable. The wind induces it. From this follows a procedure as shown in Fig. 5.6. The rotor of the turbine starts out perpendicular to the inflow wind direction. With time, the turbine yaws due to the wind force. With the yaw comes a change in force distribution. The thrust force F_T, formerly aligned with the x-axis, now has a y-component $F_{T,y}$. During the ongoing simulation, yaw and $F_{T,y}$ increase further. Finally the force is distributed in such a way that the turbine becomes unstable. This indicates that there might be a tipping point, some force constellation that determines heavy motion.

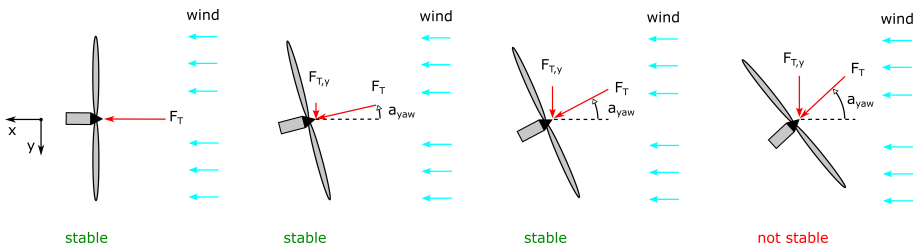

Figure 5.6.: *Roll yaw tipping*

5.3. Is there a particular force distribution when the turbine starts to pitch and roll heavily?

It turns out there is, at least for the three higher wind speeds $v_0 = 17, 20, 25\text{m/s}$. This can be seen in Fig. 5.7. Here, extreme oscillation always starts at a y-component of the thrust force $F_{T,y} \approx 400\text{kN}$. This is remarkable as it indicates that the thrust force distribution really is the reason for the observed motions.

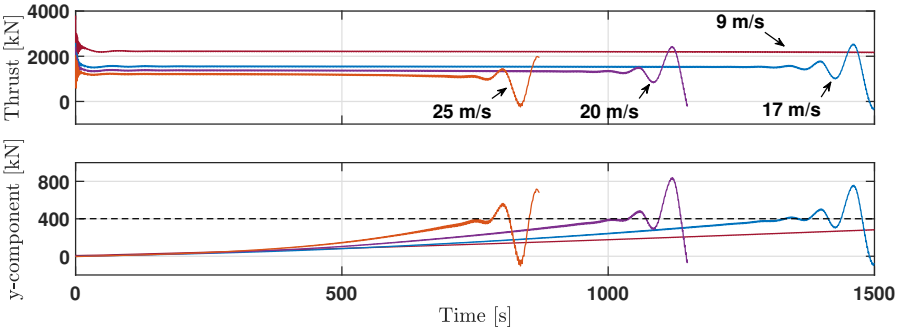

Figure 5.7.: *Total thrust force F_T and its part parallel to the y - axis. The turbine breaks into an unstable state for a thrust force in y - direction $F_{T,y} \approx 400\text{kN}$. Higher wind speeds reach this points earlier.*

But what happens with the remaining wind speed $v_0 = 9\text{m/s}$? Did we reach stability here? When we extend the simulation time to $t = 7500\text{s}$ as in Fig. 5.8, a new behaviour is visible. After crossing the value of $F_{T,y} \approx 400\text{kN}$, the turbine is destabilized. But the thrust force starts to oscillate around a stable value with $F_{T,y} \approx 400\text{kN}$. The same effect is seen in the yaw motion in Fig. 5.9 where the turbine stabilizes around a fix yaw angle. This shows that stable states are possible.

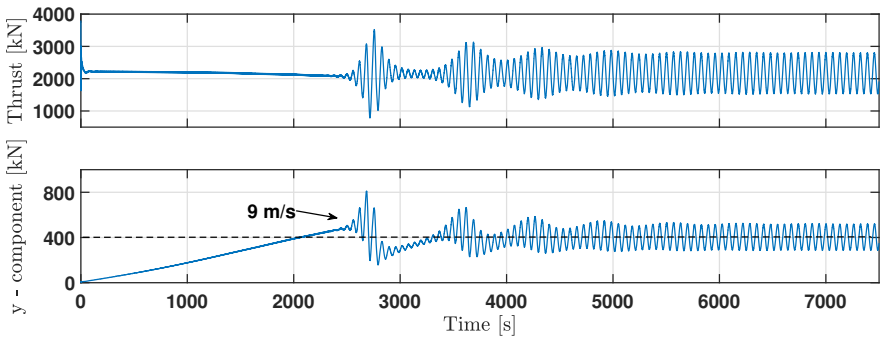

Figure 5.8.: *Total thrust force F_T and its part parallel to the y - axis for $t = 7500\text{s}$. $F_{T,y}$ crosses the value of 400kN first, then the turbine gets unstable. Remarkably, the turbine stabilizes again around $F_{T,y} \approx 400\text{kN}$.*

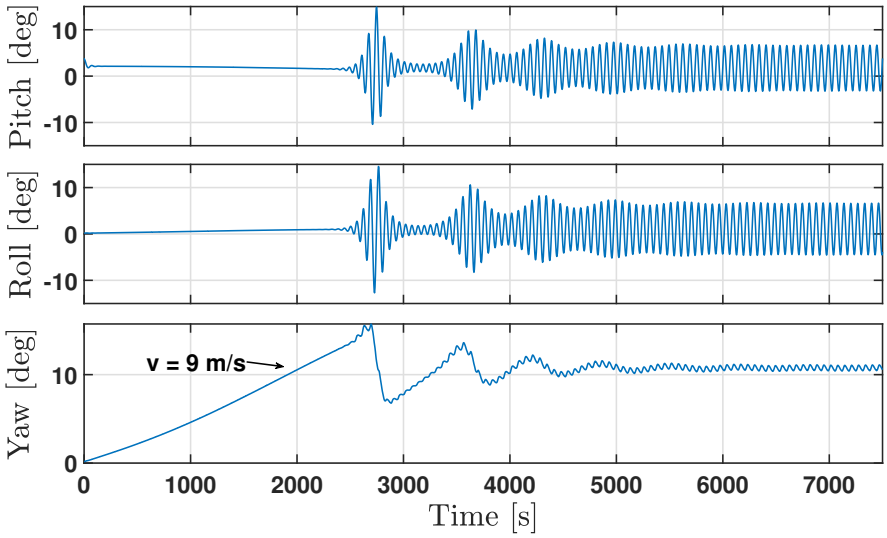

Figure 5.9.: *Movement of the turbine under wind load over $t = 7500s$. After steep increase and destabilization, the yaw balances around $\alpha_{yaw} \approx 10.75°$. Pitch and roll show heavy oscillation when the yaw motion is negative. They both stabilize in an angle slightly above 0. The turbine is in a stable motion.*

5.4. Can you prevent the instability in theory and practice?

Now that we know the reason for the heavy pitch and roll behaviour, we can go on and fix the problem. It turns out that we only have to keep $F_{T,y}$ under a certain value. For this design it amounts to $F_{T,y} \leq 400kN$. The exact value will probably differ for each substructure design.
There are two obvious ways to reduce $F_{T,y} = F_T \cdot \sin \alpha_{yaw}$. The first is to reduce F_T which can be done by blade pitching. Of course this will reduce the rotor speed and therefore the power output. The second way is to keep α_{yaw} in a certain range. With the attached cylinders, it is possible to yaw the nacelle towards the wind without destabilizing the platform, even under wind load. These conditions can be implemented into the controller of the turbine. Now the sailing turbine can be stabilized through the controller.
Finally we want to complete the platform design by including the full hydrodynamic and inertia calculations into the model.

5.5. How is the system behaving with the completed model?

The hydrodynamic modelling program AQWA (ANSYS ™ [b]) is used to calculate a new platform model. The geometry file to create the modified SPAR design in Mechanical APDL (ANSYS ™ [a]) is attached in appendix A. It creates the geometry as shown in Fig. 5.10. The four installed cylinders are no longer considered without mass. Instead we assume the cylinders with a wall thickness of $t = 0.5\text{m}$, made out of concrete with density $\rho = 2500\text{kg/m}^3$. The computed inertia and mass properties are listed in Tab. 5.1. As the cylinders create more buoyancy, ballast mass is added to keep the buoyancy level the same. The moment of inertia I_{ZZ} increases by more than four times compared to the initial SPAR design.

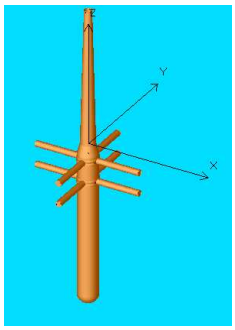

Figure 5.10.: *AQWA model geometry of the adapted SPAR platform.*

Moment of Inertia I_{XX}	$1.864 \times 10^{11}\text{kgm}^2$
Moment of Inertia I_{YY}	$1.864 \times 10^{11}\text{kgm}^2$
Moment of Inertia I_{ZZ}	$8.081 \times 10^{9}\text{kgm}^2$
Extra ballast mass m_{bal}	$6.730 \times 10^{5}\text{kg}$
Total platform mass m_{tot}	$4.635 \times 10^{7}\text{kg}$
Center of Gravity z_{grav}	-89.60m

Table 5.1.: *Mass and inertia parameters for the developed design. The ballast mass is adapted to keep the platform at the same buoyancy level. For the cylinders with a wall thickness of* $T = 0.5\text{m}$*, concrete with* $\rho = 2500\text{kg/m}^3$ *is used. The moment of inertia* I_{ZZ} *increases by more than four times compared to the initial SPAR design. Acceptable is the rise center of gravity* z_{grav} *by almost* 9m.

A re-run of earlier simulations reveals that the new AQWA model has very little impact on the turbine movements. A comparison of the movements calculated by use of the new and old model is shown in Fig. 5.11. Instabilities for both simulations occur at the same time for each wind speed respectively.

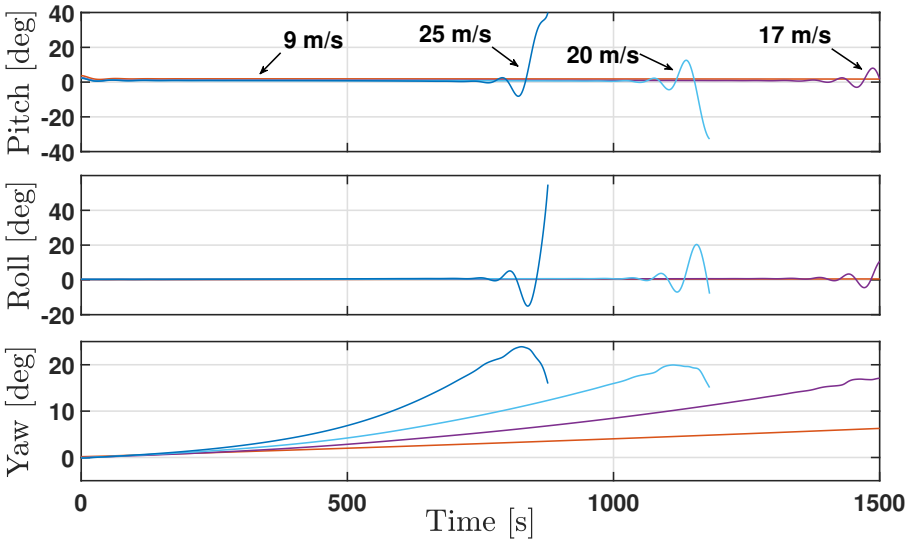

(a) *Cylinders included in AQWA model*

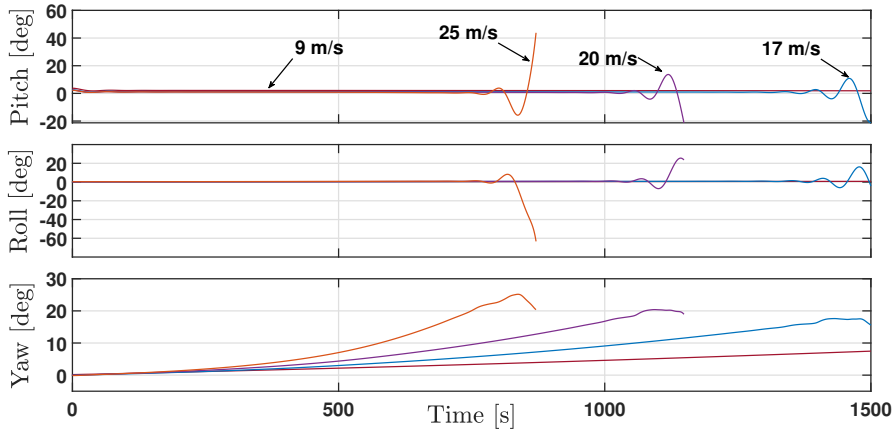

(b) *Cylinders modeled by drag force only*

Figure 5.11.: *Comparison of movements of the two AQWA platform models. Instabilities in a) and b) occur at the same time for each wind speed respectively. The more accurate calculation of hydrodynamic forces and inertia in a) did not change the result by much. Therefore, using the drag force only as in b) is a good approximation.*

The thrust force in Fig. 5.12 confirms the impression that the results are alike. Again, instability appears at a y - component of $F_{T,y} = 400kN$. For the long simulation over $t = 7500$s of the wind speed $v = 9$m/s, outcomes are also similar to calculations with the old model. These results are displayed in Fig. 5.13 and 5.14. The resemblance of the results justifies our approach to neglect many calculations in the beginning and only concentrate on the drag force. As we see, this was a good approximation.

Throughout this chapter, we have described the reason for the simulation failure and how it can be avoided. With this knowledge, a controller can be developed to prevent unstable conditions. In addition, the new platform, its properties and the acting hydrodynamic forces were computed more accurately.

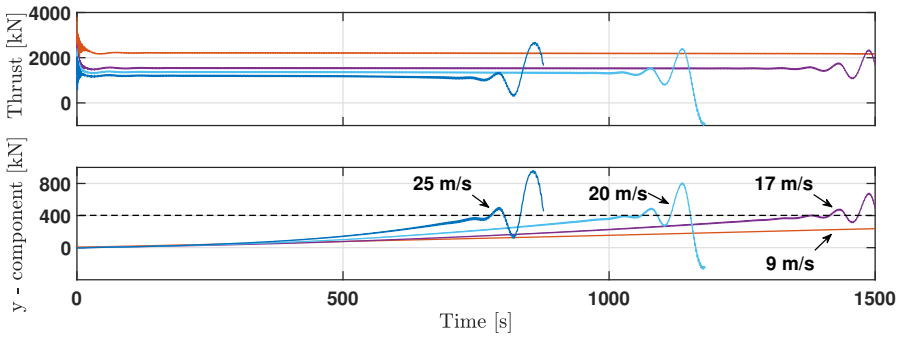

Figure 5.12.: *Total thrust force F_T and its part parallel to the y - axis. The new AQWA model calculates the hydrodynamic forces, the mass and inertia more accurately. The results are similar to earlier simulations where only the hydrodynamic drag force was considered.*

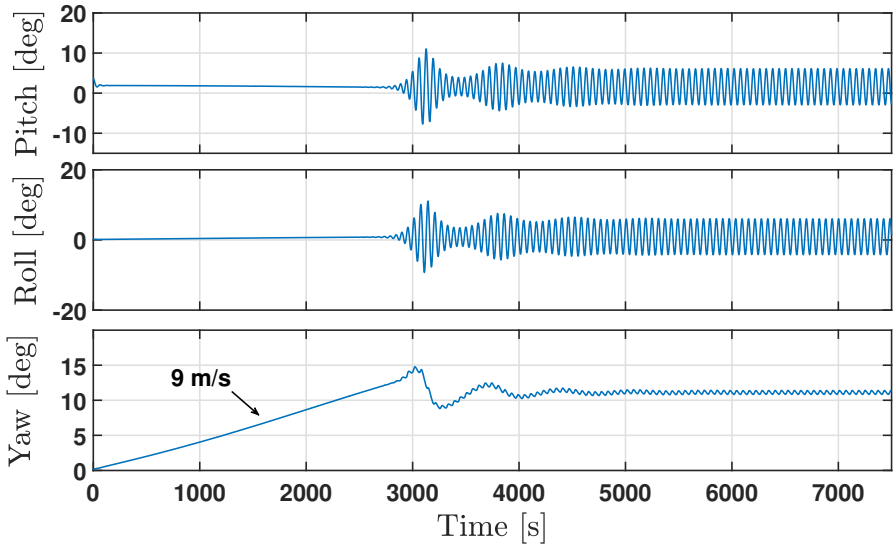

Figure 5.13.: *Movement of the turbine under wind load for* $t = 7500$s. *The new AQWA model calculates the hydrodynamic forces, the mass and inertia more accurately. The results are similar to earlier simulations where only the hydrodynamic drag force was considered.*

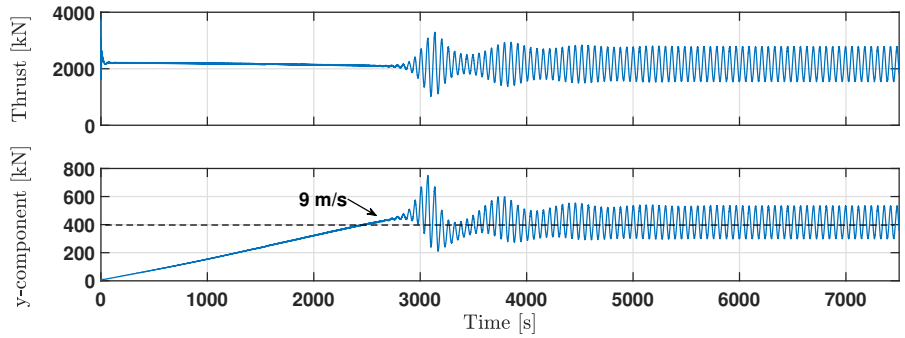

Figure 5.14.: *Total thrust force* F_T *and its part parallel to the* y *- axis for* $t = 7500$s. *The new AQWA model calculates the hydrodynamic forces, the mass and inertia more accurately. The results are similar to earlier simulations where only the hydrodynamic drag force was considered.*

Chapter 6.

Conclusion and Outlook

6.1. Conclusion

The concept of a sailing offshore wind turbine is presented. In ideal conditions, it reaches a power production competitive to traditional concepts. The meaning of this finding is limited as the turbine will encounter many non-ideal situations. A spar platform as basis for the sailing turbine is very unstable. The moment induced by the nacelle yaw motor is enough to cause heavy platform rotation. Wind load also leads to a strong yaw.
A more stable platform is developed by the attachment of drag elements. They effectively slow down the yaw speed. Nacelle – induced yaw is restricted by this, as the motor moment only acts for a defined period. Wind-induced yaw is slowed down but not restricted as the wind force acts continuously.

Great instabilities are likely to be caused by the sideway thrust force $F_{T,y}$. As the turbine yaws out of the wind inflow direction, the lateral component of the thrust force grows. Instability occurs when $F_{T,y}$ reaches a tipping point. Strong pitch and roll motions follow in which the turbine swings forth and back. For high wind speeds, the rotor blades even touch the water surface. For lower wind speeds, the turbine is able to recover and stabilize again. Limits to this hypothesis are set by the assumption that $F_{T,y} = F_T \cdot \sin \alpha_{yaw}$ is only valid for small yaw angles while we encounter great yaw angles.

6.2. Outlook

The next step is to implement the suggestions made into the model‘s control strategy. A controller that keeps the turbine stable under wind load can then be adapted to include steering manoeuvres.
The current model relies on drag cylinders with an unrealistic drag coefficient of $c_d = 100$. These should be replaced with newly designed, realistic to manufacture drag elements that develop an equivalent drag force.

On a broader view, the question of how to store the produced electric power remains open. The drag elements could be utilized to contain hydrogen tanks or batteries. A concept to retrieve the stored energy periodically from the roaming turbine needs to be developed. Also, an analysis of deployment locations and profitability is necessary.

Appendix A.

AQWA Model: ANSYS input file

```
/CLEAR
/PREP7
/UNITS,SI
*AFUN,DEG
et,1,181

r1=6.5/2
r2=13.2/2
r3=18.6/2
r4=5.0/2

k,1,0,0,129.495
k,2,0,0,0
k,3,0,0,-10
k,4,0,0,-145.7
k,5,0,0,-155
k,6,50,0,-15 !circle middle points attached cylinders
k,7,0,0,-15
k,8,0,50,-15
k,9,50,0,-35
k,10,0,0,-35
k,11,0,50,-35
k,12,55,0,-15 !help points for circle axis
k,13,0,-5,-15
k,14,-5,0,-35
k,15,0,55,-35

circle,1,r1,,,90,1
circle,2,r2,,,90,1
circle,3,r3,,,90,1
circle,4,r3,,,90,1 !Keypoint 23


circle,6,r4,12,10,180,2 !cylinder tops
circle,7,r4,6,10,180,2

circle,8,r4,7,11,180,2
circle,7,r4,13,11,180,2
```

```
circle,9,r4,10,6,180,2
circle,10,r4,14,6,180,2

circle,10,r4,11,8,180,2
circle,11,r4,15,8,180,2 !Keypoint 47

l,16,18 !SPAR hull !Line No. 21
l,17,19
l,18,20
l,19,21
l,20,22
l,21,23
l,24,27 !attached cylinders !Line No. 27
l,26,29
l,36,39
l,38,41
l,30,33
l,32,35
l,45,42
l,47,44
l,26,24 !help lines to draw cylinder surface area
l,27,29
l,25,28
l,32,30
l,31,34
l,36,38
l,37,40
l,42,41
l,45,47
l,46,43

al,1,21,2,22 !SPAR hull
al,2,23,3,24
al,3,25,4,26

al,5,6,35 !dummy cylinder surfaces
al,6,28,8,37
al,5,27,7,37
al,38,9,10
al,10,32,12,39
al,9,31,11,39
al,13,29,15,41
al,14,30,16,41
al,40,13,14
al,19,33,17,44
al,20,34,18,44
al,19,20,43

ainp,3,5,6,8,9,10,11,13,14  !create correct cylinder surfaces
nummrg,kp
l,61,32
```

```
l,60,31
l,63,30
l,65,45
l,64,46
l,67,47
l,52,26
l,53,25
l,54,24
l,56,36
l,57,37
l,58,38
al,53,4,10,7
al,54,7,9,8
al,55,11,19,12
al,56,12,20,15
al,49,17,6,16
al,50,18,5,17
al,51,26,13,25
al,52,27,14,26

circle,29,r3,,,90,1 !create correct SPAR surface
circle,7,r3,,,90,1
circle,27,r3,,,90,1
circle,39,r3,,,90,1
circle,10,r3,,,90,1
circle,41,r3,,,90,1
circle,4,r3,,,90,1
l,21,61
l,20,52
l,44,65
l,54,56
l,67,69
l,62,68
lcsl,29,53
lcsl,63,49
lcsl,32,55
lcsl,63,51
nummrg,kp
al,3,57,28,58
al,28,53,65,49
al,65,54,30,50
al,30,59,31,60
al,31,55,67,51
al,67,56,33,52
al,33,61,34,62

wpoffs,0,0,-145.7 !SPAR bottom
sphere, 0, r3, 0, 90
rectng, 0, 2*r3, 0, 2*r3
vsba, 1, 25,DELETE,DELETE
vdele, 3, , , 1
```

```
agen, 2, 26, , , , , , , 0
vdele, 2, , , 1
wpoffs,0,0,145.7

areverse,all
areverse,5,0
areverse,15,0
areverse,8,0
areverse,10,0
areverse,4,0
areverse,13,0
areverse,12,0
areverse,22,0
accat,all


! Mesh
esize,0.5,all
aesize,all,0.5
lesize,all,0.5,,,,,,,
kesize,all,0.5,,
mshape,0,2d
mshkey,2
amesh,all,,1

ANSTOAQWA,WindCrete15MW_4C,z,9.81,1025,1,1,,
```

Acknowledgement

I thank Prof. Dr. Po Wen Cheng for the possibility to do my research thesis at the Stuttgart Wind Energy resort at the Institute of Aircraft Design.
Many thanks to my supervisors Youssef Mahfouz and Andy Clifton for their support, insight and availability. I learned a great deal about organizing my own research. You always nudged me back on track when I needed it.

Erklärung

Hiermit erkläre ich, dass ich die vorliegende Forschungsarbeit mit dem Titel “Concept Study of a Sailing Offshore Wind Turbine“ selbständig angefertigt habe. Es wurden nur die in der Arbeit ausdrücklich benannten Quellen und Hilfsmittel benutzt. Wörtlich oder sinngemäß übernommenes Gedankengut habe ich als solches kenntlich gemacht.

Ort, Datum Göteborg, SE 25.01.2021

Unterschrift L. Willeke

Leonard Willeke

Bibliography

ANSYS ™. Mechanical APDL, Release 19.0, a.

ANSYS ™. Aqwa, Release 19.0, b.

A. Babarit, G. Clodic, S. Delvoye, and J.-C. Gilloteaux. Exploitation of the far-offshore wind energy resource by fleets of energy ships – part 1: Energy ship design and performance. *Wind Energy Science*, 5(3):839–853, 2020. doi: 10.5194/wes-5-839-2020. URL `https://wes.copernicus.org/articles/5/839/2020/`.

Odd Faltinsen. *Sea loads on ships and offshore structures*, volume 1. Cambridge University Press, 1993.

Evan Gaertner, Jennifer Rinker, Latha Sethuraman, Frederik Zahle, Benjamin Anderson, Garrett Barter, Nikhar Abbas, Fanzhong Meng, Pietro Bortolotti, Witold Skrzypinski, George Scott, Roland Feil, Henrik Bredmose, Katherine Dykes, Matt Shields, ChristopherAllen, and Anthony Viselli. Definition of the iea 15-megawatt offshore reference wind turbine. `https://www.nrel.gov/docs/fy20osti/75698.pdf`, 2020.

Robert Gasch, Klaus Knothe, and Robert Liebich. *Strukturdynamik*. Springer, Berlin, Heidelberg, 2012.

Herbjorn Haslum, Mathias Marley, Bjorn Skaare, and Hakon Andersen. Aerodynamic roll-yaw instabilities of floating offshore wind turbines. In *Proceedings of the ASME 2020 39th International Conference on Ocean, Offshore and Arctic Engineering*. American Society of Mechanical Engineers, 2020.

Andrew Henderson, Maurizio Cullo, and Marco Masciola. Overview of floating offshore wind technologies. In Joao Cruz and Mairead Atcheson, editors, *Floating Offshore Wind Energy*, pages 87–132. Springer, Lisbon, Portugal, 2016.

J.M.J. Journee and W.W. Massie. *Offshore Hydrodynamics*. Delft University of Technology, 2001.

Youssef Mahfouz, Mohammad Salari, Fernando Vigara, Sergio Hernandez, Climent Molins, Pau Trubat, Henrik Bredmose, and Antonio Pegalajar-Jurado. D1.3. Public design and FAST models of the two 15MW floater-turbine concepts, December 2020. URL `https://doi.org/10.5281/zenodo.4385727`. This deliverable is a draft version, and still under revision by the EC.

James Manwell, Jon McGowan, and Anthony Rogers. *Aerodynamics of Wind Turbines*, chapter 3, pages 91–155. John Wiley Sons, Ltd, 2009.

NREL ™. OpenFAST, V2.4.0. URL `https://www.nrel.gov/wind/nwtc/openfast.html`.

Ken Schwaber and Jeff Sutherland. The Scrum Guide ™, November 2017. URL `https://www.scrumguides.org/`.

B. Skaare. Development of the hywind concept. In *Proceedings of the ASME 2017 36th International Conference on Ocean, Offshore and Arctic Engineering*. American Society of Mechanical Engineers, 2017.

Jean-Pierre Vidal. System for propulsion of boats by means of wind and streams and for recovery of energy, U.S. Patent 4 371 346, Aug. 1980.